When modified to include the effect of the unequal weighting of the events, the unnormalized likelihood function for a given σ_i is

$$\mathfrak{L}(\sigma_i)=\prod_{j=1}^{n}(f_{ij})^{w_j},$$

where the weight of the given event w_j is the reciprocal of the detection probability of the event, and n is the total number of events in the region. The resulting likelihood function correctly locates the most probable value of σ, but its width will be too narrow by a factor

$$[(\sum_{j=1}^{n} w_j^2)/n]^{1/4},$$

since the inclusion of the weights of the events in the manner described has artificially narrowed the likelihood function to a width appropriate to a number of events $\sum_{j=1}^{n} w_j$, rather than to the actual number n.

PHYSICAL REVIEW VOLUME 166, NUMBER 5 25 FEBRUARY 1968

K^+-Meson Production in p-p Collisions at 2.5–3.0 GeV *

W. J. HOGAN,† P. A. PIROUÉ, AND A. J. S. SMITH
Palmer Physical Laboratory, Princeton University, Princeton, New Jersey
(Received 24 August 1967)

Differential cross sections as a function of momentum are presented for the production of K^+ mesons in p-p collisions at incident proton energies of 2.54, 2.88, and 3.03 GeV. The measurements were made at 20°, 30°, and 40° relative to the direction of the internal proton beam of the Princeton-Pennsylvania accelerator. At 2.54 GeV, the results follow closely the predictions from phase space (with 60% $K^+\Sigma N$ and 40% $K^+\Lambda p$ in the final state). At 2.88 and 3.03 GeV, however, there is a definite disagreement with phase space. The data are compared to the predictions of three models: (1) a model based on the assumption that K's are produced via $p+p\rightarrow K^++X^+$, where X^+ is a $B=2$, $S=-1$ resonance which decays into a nucleon+hyperon; (2) the isobar model; and (3) the one-pion-exchange model. Model (1) is found to be inconclusive, model (2) is inadequate, and model (3) is partly successful in predicting total cross sections, but not in interpreting the *detailed* experimental observations.

I. INTRODUCTION

IN this paper we present the results of an experimental study of K^+-meson production in p-p collisions at 2.5–3.0 GeV. One of the objectives of this study was to investigate a departure from phase space which had been noticed previously[1] in the momentum distribution of K^+ mesons produced at 30° in the laboratory by 2.9-GeV protons striking a beryllium target. One of us (P. A. P.) speculated[2] that this effect could be attributed to a resonance with baryon number 2 and strangeness -1 at a mass of about 2.36 GeV/c^2. Another objective was the determination of K^+-production cross sections in this energy range to an accuracy sufficient to permit a comparison with various theoretical models.

Previous data on strange-particle production in p-p interactions at $\sim$3 GeV come, apart from very early measurements,[3] from a bubble-chamber experiment by Louttit *et al.*,[4] and a counter experiment by Melissinos *et al.*[5] The bubble-chamber data, although of limited statistical accuracy, are most useful in giving an estimate for the relative contribution of the different channels leading to a K^+ in the final state, i.e., $K^+\Lambda p$, $K^+\Sigma N$, and $K^+YN\pi$. In the counter experiment, the momentum spectra of K^+ mesons produced at 0° and 17° in the laboratory were obtained for incoming proton energies of 2.85 and 2.40 GeV. The 0° data show a narrow peak at the upper end of the K^+ momentum spectrum. It was speculated that this singularity could be caused by a bound state of the Λp system, a virtual system, or a resonant state.

In the present counter experiment, we have measured the momentum spectra of K^+ mesons produced at 20°, 30°, and 40° in the laboratory for incident proton energies of 2.54, 2.88, and 3.03 GeV. K^+ mesons, produced in a liquid-hydrogen target located inside the vacuum chamber of the Princeton-Pennsylvania accelerator (PPA), were identified by mass analysis.

* This work was supported by the U. S. Office of Naval Research Contract No. N0014-67-A-0151-0001.
† Present address: Lawrence Radiation Laboratory, University of California, Livermore, Calif.
[1] P. A. Piroué and A. J. S. Smith, Phys. Rev. **148**, 1315 (1966).
[2] P. A. Piroué, Phys. Letters **11**, 164 (1964). Due to an error in the beam calibration the *absolute* value of the K^+-meson cross sections reported in this paper are overestimated by a factor $\sim$6. This has, however, no bearing on the conclusions of the paper.
[3] R. L. Cool, T. W. Morris, R. R. Rau, A. M. Thorndike, and W. L. Whittemore, Phys. Rev. **108**, 1048 (1957); P. Baumel, G. Harris, J. Orear, and S. Taylor, *ibid.* **108**, 1322 (1957); D. Berley and G. B. Collins, *ibid.* **112**, 614 (1958).
[4] R. I. Louttit, T. W. Morris, D. C. Rahm, R. R. Rau, A. M. Thorndike, W. J. Willis, and R. M. Lea, Phys. Rev. **123**, 1465 (1961).
[5] A. C. Melissinos, N. W. Reay, J. T. Reed, T. Yamanouchi, E. Sacharidis, S. J. Lindenbaum, S. Ozaki, and L. C. L. Yuan, Phys. Rev. Letters **14**, 604 (1965).

In the next section we describe the experimental arrangement including the target, the monitors, and the method of detecting K^+ mesons. The experimental results are presented in Sec. III and discussed in Sec IV. Finally, a summary and conclusions are presented in Sec. V.

II. EXPERIMENTAL ARRANGEMENT

A. Hydrogen Target and Monitors

As the PPA had no external proton beam at the time of the experiment, we used a liquid-hydrogen target located inside the vacuum chamber of the synchrotron. This target has been described in detail elsewhere,[6] so it will be discussed here only briefly. Except for a modification required to protect the target cup from the 3-MeV injected protons, our target assembly was similar to a Cambridge electron accelerator design[7] in which liquid hydrogen is obtained by circulating cold helium gas through a heat exchanger. The liquid hydrogen dropped into a cylindrical target cup, $3\frac{1}{2}$ in. high and $\frac{1}{2}$ in. in diameter. The target walls were made of $\frac{1}{2}$-mil-thick H Film, a polyimide film similar to Mylar but much more resistant to radiation. Although the heat input due to the 3-GeV protons was negligible, the target could not dissipate the energy deposited by the 3-MeV injected protons. Therefore, a rotating aluminum shutter, $\frac{1}{4}$ in. thick, was used to shield the target cup from the proton beam at injection time. At 3 GeV, the circulating protons traversed the target about five times before striking a massive dump target placed at a proper radius 90° upstream. By comparing the known[8] cross section for π^+ production in 2.9-GeV p-p collisions with our data taken at 30° laboratory angle, we found that the effective target thickness as seen by the beam was 0.30–0.35 g/cm^2 of hydrogen.

The incident proton beam striking the hydrogen was continuously monitored with a scintillation counter arrangement S_7S_8 (Fig. 1) located in a momentum-analyzed beam at 60° and tuned for the elastically scattered protons from free protons at that angle. As seen in Fig. 2, the elastic peak, so prominent when incident protons strike hydrogen, is completely washed out when another target material is used, e.g., beryllium. It can be shown[1] that Fermi motion (motion of nucleons bound in the nucleus) accounts for the disappearance of the elastic peak at this angle. The scattered protons, identified by momentum analysis and time-of-flight techniques, were signaled at the elastic peak by the coincidence S_7S_8, and at the valley between the elastic and inelastic peaks by the coincidence S_7S_{10}. The peak-to-valley ratio, normally of the order of 10, was a very sensitive indicator of whether the whole incident proton beam was striking hydrogen.

As a further check the relative intensity of the beam striking the target was also monitored by a three-counter telescope (M) located on the 75° line.

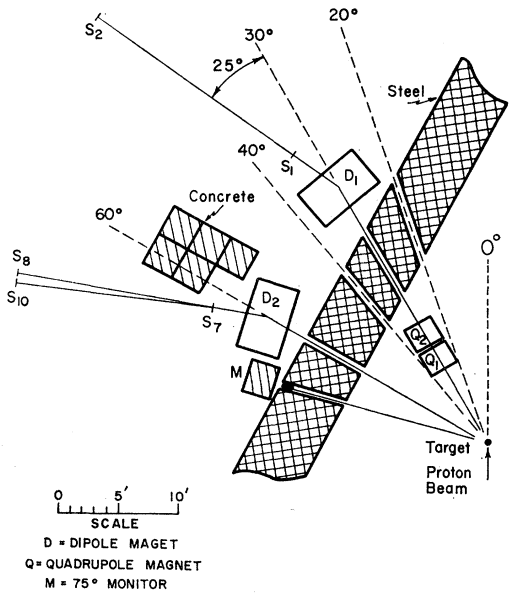

FIG. 1. Layout of the beams.

B. K-Meson Detection

Figure 1 shows the layout of the beams. The target could be viewed through five channels located at 20°, 30°, 40°, 60°, and 75° relative to the direction of the PPA internal proton beam. Except for the 60° and 75° channels which were used to monitor the beam on target, as explained above, each beam consisted of a quadrupole doublet Q_1-Q_2, a dipole magnet D_1, and two scintillation counters S_1 and S_2. The distance between S_1 and S_2 was 10 ft for measurements in the momentum range 350–

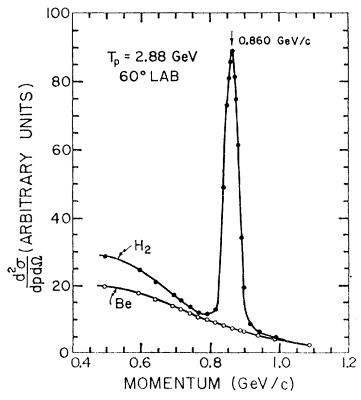

FIG. 2. Momentum spectra of protons emitted at 60° lab from hydrogen and beryllium targets struck by 2.88-GeV protons.

[6] W. J. Hogan, R. Jankowicz, P. A. Piroué, and F. C. Shoemaker, IEEE Trans. Nucl. Sci. **12**, 251 (1965).

[7] L. Hand, J. Rees, W. Shlaer, J. K. Walker, and R. Wilson, *Nucleon Structure* (Stanford University Press, Stanford, Calif., 1964), p. 364.

[8] A. C. Melissinos, T. Yamanocuhi, G. G. Fazio, S. J. Lindenbaum, and L. C. L. Yuan, Phys. Rev. **128**, 2373 (1962).

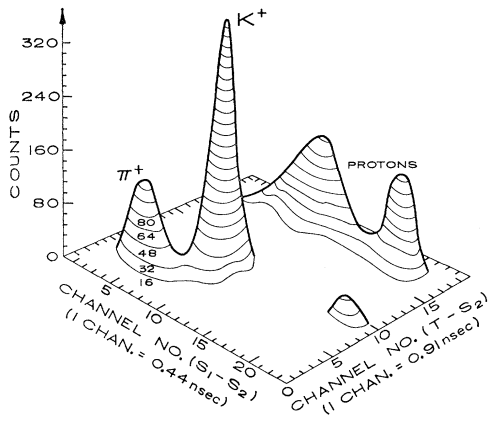

FIG. 3. Two-dimensional distribution of times-of-flight for a 1-GeV/c positive beam. T-S_2 represents the time-of-flight from the target to S_2, 50 ft away; S_1-S_2 is the time-of-flight between S_1 and S_2, 20 ft apart. The contour lines give the number of counts. As explained in the text most protons and pions were purposely rejected. The structure in the proton shoulder and the small extraneous bump come from coherent accidental coincidences, and do not affect the K measurement.

800 MeV/c, and 20 ft for those in the range 500–1300 MeV/c. Thus the overlapping region provided a means of normalizing one curve to the other. S_1 was 1 in. wide, 2 in. high, and $\frac{1}{8}$ in. thick; S_2, 2 in. wide, 5 in. high, and $\frac{1}{4}$ in. thick. The scintillation material was Pilot B. Helium bags were used wherever possible.

K^+ mesons were identified by mass analysis. The momentum was selected by magnetic deflection and the velocity determined by time-of-flight measurements made between the two counters S_1 and S_2, *and also* between one of the counters and the target. The technique of time-of-flight measurements from the target[9] takes advantage of the rf structure of the PPA internal proton beam. The two times of flight were converted into pulse heights and then fed into a two-dimensional pulse-height analyzer. Figure 3 shows a two-dimensional time-of-flight distribution for a run at 1 GeV/c. In order to make sure that K^+ mesons were detected with full efficiency, the coincidence requirements were always such that small portions of the π^+-meson and proton peaks were retained. This method has the advantage of eliminating any momentum dependence of the K-detection efficiency while keeping the background at an acceptable level (less than 1% in most cases). At low momenta (below ~550 MeV/c) we found it necessary to eliminate protons by stopping them in a copper absorber placed in front of S_2. In Sec. III B we explain how we corrected the data for this effect.

For the momentum calibration we used the difference between the π^+-meson and proton times of flight. Although the presence of quadrupoles modifies the solid angle and the momentum resolution, it leaves the shape of the momentum spectra unaltered. Therefore, Q_1-Q_2 were tuned by maximizing the K^+ rate at a given momentum; a linear relationship between momentum and applied current was then used for other values.

Our primary aim in this experiment was to determine the shape of the K^+ momentum spectra. Yet, we were also able to find absolute cross sections for K^+ production relative to π^+ production by counting simultaneously the number of π^+ mesons which passed through the detector. This was done simply by setting up, parallel to the K electronics system, a time-of-flight circuit tuned for π mesons. An absolute normalizing factor is then easily found by comparing the π^+ spectra with known data.[8]

III. EXPERIMENTAL RESULTS

A. Laboratory Spectra

K^+ momentum spectra were measured at 20°, 30°, and 40° laboratory angles with an incident proton energy of 2.54 GeV; at 20° and 30° with an energy of 2.88 GeV; and at 30° with an energy of 3.03 GeV. At each angle and proton energy we covered the spectrum several times throughout the four-week running period; a weighted average was then taken at each momentum. The statistical uncertainties affecting these averages are in general of the order of 1%. The data were corrected for (a) background, (b) K^+ decay, (c) nuclear absorption, (d) multiple scattering and losses in the copper when applicable, (e) dead-time losses in the pulse-height analyzer, and (f) nonhydrogen events. These corrections are described below.

The corrected data are shown in Fig. 4 and summarized in Table I. The indicated errors include the statistical errors as well as the uncertainty introduced through the application of the above corrections; but they do not include the uncertainty in the absolute calibration which amounts to ~16%. This uncertainty mainly comes from that affecting the π^+ data[8] to which we compared our own π^+ data.

The uncertainty in the momentum scale is about 1.7% while the momentum resolution ($\Delta p/p$) ranged from 1.5% at 20° to 3% at 40°.

In Fig. 4 the solid line is merely intended to be a guide to the eye; it does not represent any mathematical fit. The dashed curve represents the expectation from phase space normalized to the area under the solid line; each case is discussed in detail in Sec. IV.

B. Corrections

(a) The background, as estimated directly from the output of the two-dimensional pulse-height analyzer, was subtracted from the number of kaons counted. It was usually less than 1%.

(b) The correction for K^+ decay is straightforward. However, it was so large (a factor ~7 at 1000 MeV/c, ~25 at 500 MeV/c) that a detailed calculation was necessary to estimate the fraction of kaons whose

[9] P. A. Piroué and A. J. S. Smith, Report No. PPAD-2137-545, Princeton-Pennsylvania Accelerator, Princeton University, 1965 (unpublished); see also IEEE Trans. Nucl. Sci. 12, 249 (1965).

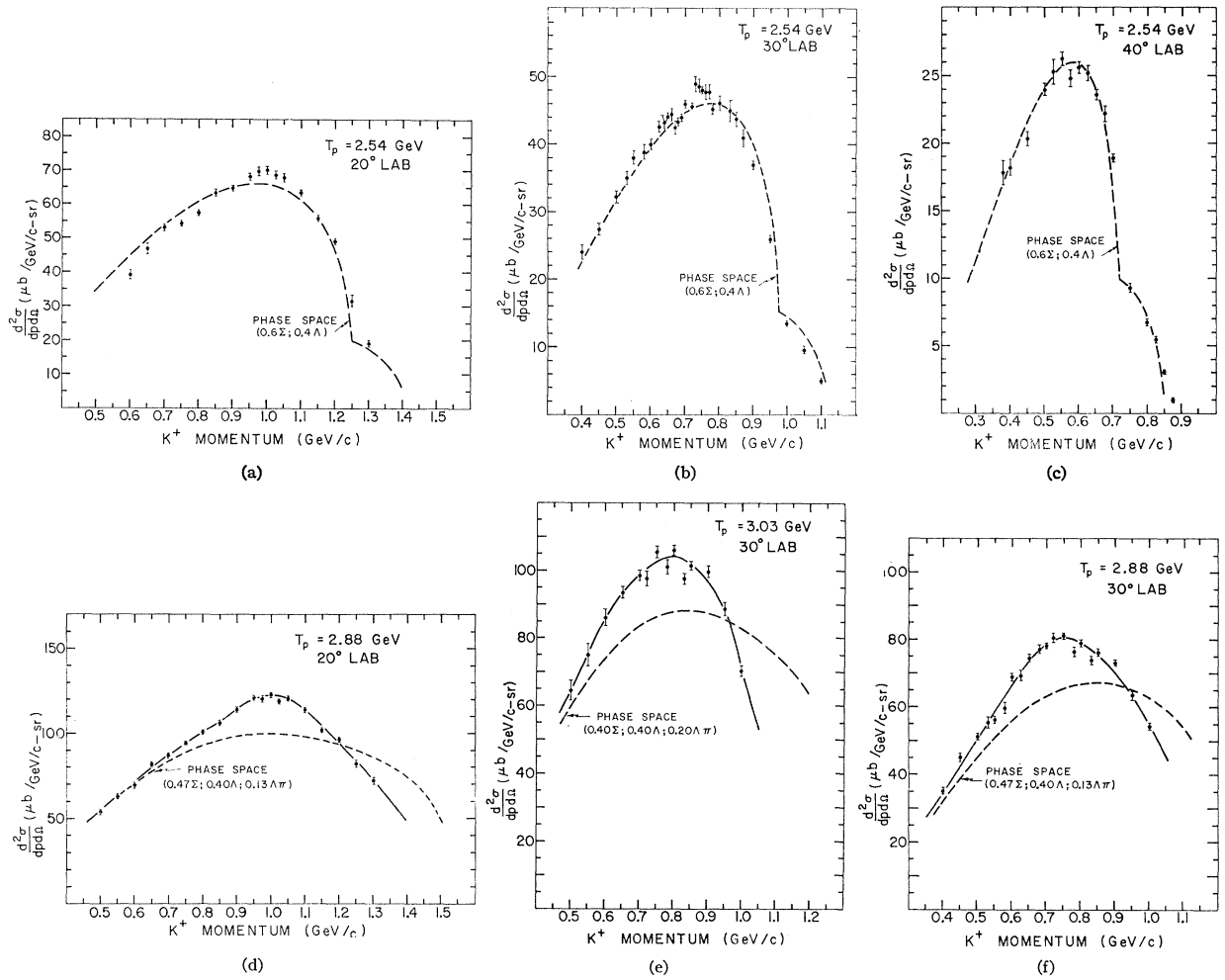

FIG. 4. Laboratory momentum spectra of K^+ mesons produced in hydrogen at the lab angles and incident proton kinetic energies indicated. Errors include statistical errors as well as uncertainties introduced through corrections, but do not include the ~16% uncertainty in the absolute calibration. Momentum resolution is ~2%. The dashed lines represent phase space (see text) normalized to the area under the data.

charged decay products were mistaken for undecayed kaons.

(c) Nuclear absorption in the air, helium, and S_1 amounted to less than 2.5%, and, to first order, was independent of the momentum in the range of interest.

(d) The loss due to interactions (nuclear and Coulomb) in the copper absorber placed directly in front of S_2 was found experimentally at intermediate momenta (~550–650 MeV/c) by taking runs with and without copper absorber. The over-all correction factor (~10%) was then extrapolated to the lower momenta at which it was difficult to take runs without copper. We made calculations similar to those of Sternheimer[10] to estimate the loss due to multiple scattering.

(e) The correction due to dead time of the analyzer is straightforward. It generally amounted to ~5%.

(f) The correction for K^+ mesons produced in materials other than hydrogen (mainly the target walls) could be extracted from the momentum spectrum shown in Fig. 5. In this spectrum, obtained at 40° and 2.54 GeV, the data, duly corrected except for non-H_2 events, follow the phase-space curve quite well up to the kinematical cutoff, but then extend in a long tail beyond the cutoff. Since these kaons cannot be produced without some target motion, they must have originated in materials other than hydrogen. Therefore, this tail was fitted to a phase-space curve in which the effects of Fermi motion have been included. Integrating this curve over the whole spectrum, we found that the nonhydrogen events constituted about 10% of the total. This fraction was used in all other spectra. The actual correction depended, of course, on momentum, angle, and incident energy. It ranged from 7–10% at low and medium momenta to over 90% at the high-momentum cutoffs.

[10] R. M. Sternheimer, Rev. Sci. Instr. **25**, 1070 (1954).

TABLE I. Differential cross sections in the laboratory system for K^+ mesons produced in p-p collisions at the incident proton energies indicated. The K^+ production angles are given in the laboratory system. Errors include statistical errors and the uncertainty introduced through corrections, but do not include the ~16% uncertainty in the absolute calibration.

	$d^2\sigma/dpd\Omega$ [μb/(GeV/c)sr]					
P_K(lab) (GeV/c)	2.54 GeV 20°	30°	40°	2.88 GeV 20°	30°	3.03 GeV 30°
0.380			17.8 ±0.9			
0.400		24.0 ±1.1	18.2 ±0.6		35.0±1.0	
0.450		27.4 ±0.9	20.3 ±0.6		45.0±1.2	
0.500		32.2 ±0.9	24.0 ±0.4	53.7±1.6	51.2±1.0	64.5±2.8
0.525			25.3 ±0.9			
0.530		35.0 ±1.0			55.3±1.7	
0.550		38.0 ±1.0	26.2 ±0.5	62.7±1.6	56.1±1.1	75.0±3.3
0.575			24.8 ±0.6			
0.580		38.8 ±1.1			59.7±1.7	
0.600	39.1±1.4	40.0 ±0.8	25.6 ±0.4	69.5±1.6	68.8±1.2	86.1±2.5
0.625		42.6 ±0.8	25.2 ±0.6		69.3±1.6	
0.640		43.3 ±1.0				
0.650	46.8±1.5	44.1 ±0.6	23.6 ±0.4	81.7±1.6	74.5±1.1	93.6±1.7
0.660		44.4 ±1.0				
0.670		42.5 ±1.0				
0.675			22.2 ±0.6			
0.680		43.3 ±0.6			77.1±1.3	
0.690		43.9 ±0.6				
0.700	53.1±0.9	45.9 ±0.6	18.9 ±0.3	86.9±1.4	78.1±0.9	98.6±1.5
0.720		45.6 ±0.6			80.5±1.4	97.7±2.2
0.730		48.9 ±1.2				
0.740		48.6 ±1.1				
0.750	54.3±0.9	48.0 ±0.6	9. 24±0.34	94.0±1.3	81.0±1.0	105.5±1.7
0.760		47.7 ±1.1				
0.770		47.7 ±1.1				
0.780		45.1 ±0.7			76.3±1.4	101.1±2.1
0.800	57.4±0.9	46.1 ±1.1	6.72±0.20	100.4±1.4	78.9±1.1	106.0±1.4
0.825			5.43±0.26			
0.830		45.0 ±1.6			73.9±1.2	97.6±1.6
0.850	63.4±1.0	43.7 ±1.1	3.06±0.15	105.9±1.4	76.2±1.1	101.5±1.3
0.870		40.9 ±1.3				
0.875			0.94±0.17			
0.900	64.7±0.8	36.9 ±0.7	0.40±0.13	113.8±1.5	73.1±0.9	99.7±1.7
0.950	68.1±1.0	26.0 ±0.6		120.8±1.5	63.4±1.3	88.7±2.0
0.975	69.7±1.4			120.1±2.0		
1.000	70.1±1.1	13.5 ±0.4		122.5±1.5	54.3±1.0	70.3±1.6
1.025	68.6±1.2			118.7±1.6		
1.050	67.8±1.2	9.64±0.57		120.4±1.5		
1.100	63.4±0.9	5.05±0.42		113.8±1.3		
1.150	55.9±0.9			101.8±1.3		
1.200	49.1±0.9			96.3±1.4		
1.250	31.6±1.7			82.1±2.1		
1.300	19.0±0.9			72.2±2.0		

C. Incident Energy

The kinetic energy of the incident proton beam was obtained by measuring the magnetic field of the synchrotron at the target radius as a function of time during the acceleration cycle. Then the incident energy was defined by gating on the electronics only for a short time interval (1 msec) at a fixed time after injection. In this way we were able to measure K^+ production in the three following energy regions: 2.54±0.02, 2.88±0.02, and 3.03±0.02 GeV.

D. Center-of-Mass Spectra

In Fig. 6, we present the momentum spectra transformed to the c.m. system. Above each curve is indicated the K^+ c.m. angles which range from 60° to 140°. There does not seem to be any anisotropy. This can be seen more clearly in Figs. 7 and 8 where we have plotted all data obtained at a given energy. It is quite clear that not only the shapes of the spectra but also the absolute values of the cross sections are the same at a given proton energy. Therefore, we conclude that within the range of this experiment there is no detectable angular dependence.

Assuming that isotropy in the c.m. system holds for the entire sphere and at all three energies, we have calculated the total cross section for K^+ production at each energy by integrating over momentum and angle. The results are shown in Table II together with theoretical predictions of the one-pion-exchange (OPE) and one-kaon-exchange (OKE) models. The indicated errors include the 16% uncertainty in the absolute cross sections as well as the uncertainty introduced by the integration over momentum (6%). Our value at 2.88 GeV (123±21 μb) agrees within statistics with that obtained by Louttit *et al.*[4] (129±20 μb) while it dis-

agrees slightly with the value reported by Melissinos *et al.*[5] (181±36 μb).

IV. INTERPRETATION OF THE DATA

A. General

The most obvious feature which is common to all our spectra is the absence of any fine structure. Although very narrow peaks cannot be excluded, any substantial structure wider than ~25 MeV/c would show. In particular, we do not observe, in the 2.54-GeV data, the narrow peak at the upper end of the momentum spectra which was reported by Melissinos *et al.*[5] However, this singularity in the Λp system, which is clearly seen in their 0° spectra, does not appear in their 17° spectra. Therefore, we would not necessarily expect to see it in our spectra since they were taken at angles larger than 17°.

Possible enhancements in the Λp system which could be attributed to a $B=2$, $S=-1$ resonance have also been reported at 2.22 GeV/c^2 by Buran *et al.*,[11] 2.36 GeV/c^2 by Piroué,[2] and 2.10 GeV/c^2 (in the Λn system) by Cohn *et al.*[12] Again in the present experiment, we find no evidence for these enhancements. However, a broad resonance ($\gtrsim$150 MeV/c^2) would show up in the momenta spectra as a very wide peak which, if the available phase space is restricted to a narrow momentum interval as it is the case at our energies, could be easily overlooked. This possibility, hereafter referred to as the dibaryon model, is examined in Sec. IV C.

In the analysis below, we first compare our momentum spectra to those predicted by phase space, and then to the predictions of three models: the dibaryon, isobar, and one-pion-exchange model.

B. Phase Space

In Figs. 4–8 the momentum spectra expected from Lorentz-invariant phase space are represented by the dashed curves, normalized to the total area under the data curves. The sharp discontinuities in the slopes near the upper end of the spectra occur at the Σ threshold.

At 2.54-GeV incident proton energy, the best fit to the data is obtained with 40% $K^+\Lambda p$ and 60% $K^+\Sigma N$ in the final state. (We have neglected four-body final states since 2.54 GeV is only slightly above the four-body threshold.) The estimated error is ±5%. We see that the agreement is quite good at this energy.

At 2.88 GeV we have used the results of Louttit *et al.*,[4] obtained at 2.85 GeV, for the relative contributions of the different channels leading to a K^+ in the final state: 40% $K^+\Lambda p$, 47% $K^+\Sigma N$, and 13% $K^+YN\pi$, where Y denotes a Σ or a Λ, and N the appropriate nucleon.

[11] T. Buran, O. Eivindson, O. Skjeggestad, H. Tafte, and I. Vegge, Phys. Letters **20**, 318 (1966).

[12] H. O. Cohn, K. H. Bhatt, and W. M. Bugg, Phys. Rev. Letters **13**, 668 (1964).

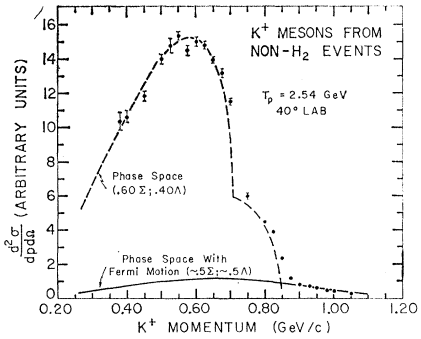

FIG. 5. Momentum spectrum used to find the fraction of kaons produced in nonhydrogen events. The dashed line represents phase space for a target nucleon at rest, while the solid line represents phase space with Fermi motion and normalized to the high-momentum tail (see text).

At 3.03 GeV we have assumed the following composition based on an interpolation between the data of Louttit *et al.*[4] and those of Bierman *et al.*[13] (obtained at 4.1 GeV): 40% $K^+\Lambda p$, 40% $K^+\Sigma N$, and 20% $K^+YN\pi$.

It is quite clear that while the agreement between data and phase space is quite good at 2.54 GeV, this is definitely not the case at the two higher energies. Also, it should be noted that at the middle of the spectra, where the deviations are large, the phase-space curves are relatively insensitive to changes in the above branching ratios. These results confirm earlier findings mentioned in Ref. 2.

C. Dibaryon Model

In this model one assumes that K^+ mesons are produced in the reaction

$$p+p \rightarrow K^+ + X^+, \qquad (1)$$

where X^+ is a $B=2$, $S=-1$ resonance which subsequently decays into a nucleon+hyperon.

One can make a rough test of the consistency of the data with this model by dividing, in the same coordinate system, the data by phase space and plotting this ratio against the invariant mass of the state X^+. Such a plot is shown in Fig. 9, for all six sets of data. The fact that the deviation from phase space appears to be localized at a well-defined X-mass region seemed to us to warrant

TABLE II. Total cross sections for K^+ produced in p-p collisions at the energies indicated compared with results of OPE and OKE calculations at 2.50, 2.85, and 3.00 GeV (see Ref. 24).

Energy (GeV)	Measured cross sections (μb)	Calculated cross sections (μb) OPE	OKE
2.54	61±10	96	182
2.88	123±21	133	361
3.03	160±29	152	449

[13] E. Bierman, A. P. Colleraine, and U. Nauenberg, Phys. Rev. **147**, 922 (1966).

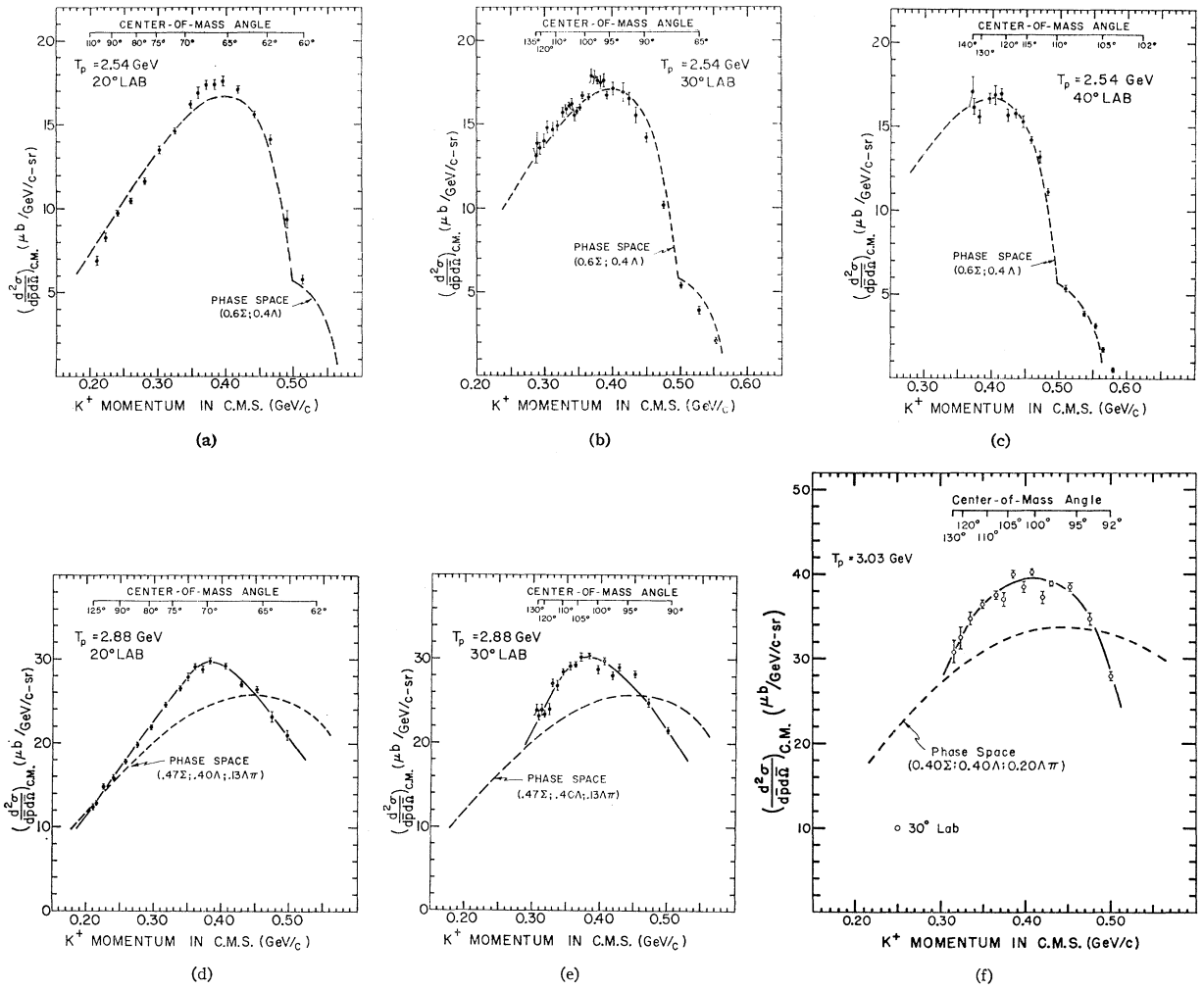

FIG. 6. Momentum spectra (shown in Fig. 4) transformed to the c.m. system.

further investigation. Consequently, we have fitted the c.m. data to a momentum distribution for K^+ of the form

$$F(p_k) \propto \left[a + A(1-a) \frac{\frac{1}{2}\Gamma}{(M-M_0)^2+\frac{1}{4}\Gamma^2} \right] \frac{d\rho_3}{dp_k}, \quad (2)$$

where $d\rho_3/dp_k$ is the three-body phase-space distribution, a the fraction of nonresonant background, and $1-a$ the fraction of events which go via (1); M_0 and Γ are the central mass and the full width at half-maximum of the state X^+, respectively. The constant A normalizes the Breit-Wigner distribution to phase space, i.e.,

$$A = \int (d\rho_3/dp_k)dp_k \Big/ \int \tfrac{1}{2}\Gamma[(M-M_0)^2+\tfrac{1}{4}\Gamma^2]^{-1} \times (d\rho_3/dp_k)dp_k.$$

The parameters to be estimated are M_0, Γ, and a. Strictly speaking, one should allow the parameter a to vary with the incoming proton energy. Therefore, there are in fact *five* parameters. The best fits are obtained with $M_0=2.38$ GeV/c^2, $\Gamma=150$ MeV/c^2, $a_{2.54}=1$, $a_{2.88}=0.7$, and $a_{3.03}=0.6$.

Needless to say, with so many parameters the available data, i.e., the c.m. spectra at the three incident proton energies [Figs. 7, 8, and 6(f)] do not constitute a very stringent test for this model. Even so, the fits are not exceptionally good, as seen in Fig. 10.

In a bubble-chamber experiment Bierman *et al.*[13] have searched for dibaryon states in p-p interactions at an incident proton energy of 4.1 GeV. For their 284 $K^+\Lambda p$ events, the Dalitz plot shows a clustering of events along a band in the ΛK system at about the mass of the $N^*(1688)$ isobar, but not along any band in the Λp system. However, within the N^* band the points seem to be more tightly clustered at a Λp mass of $\sim$2.5 GeV/c^2. This causes an enhancement with respect to phase space when the data is projected onto the Λp-mass axis, and could be the origin of the deviation from phase space exhibited by our data. In any case no firm conclusion can be drawn regarding this model.

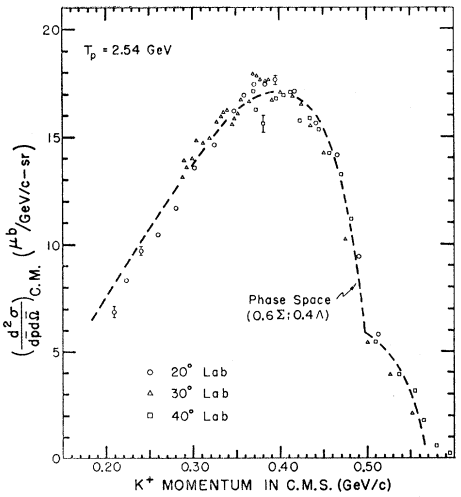

FIG. 7. Center-of-mass momentum spectrum of K^+ mesons produced at 2.54 GeV and lab angles of 20°, 30°, and 40°. For clarity only a few error bars are shown.

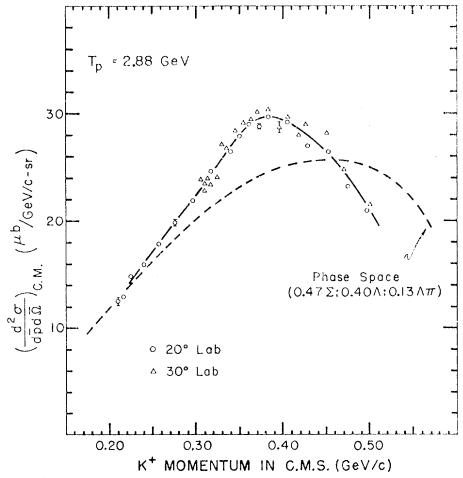

FIG. 8. Center-of-mass momentum spectrum of K^+ mesons produced at 2.88 GeV and lab angles of 20° and 30°. Again only a few error bars are shown.

D. Isobar Model

There is considerable evidence that single-pion production in 3-GeV p-p interactions proceeds via the $N_{33}^*(1236)$ isobar with a strong angular dependence ($\sim\cos^{16}\theta$) in the isobar production.[14,8] It is tempting to try to understand our data along similar lines since there is now some good evidence[13,15–18] that $N^{*+}(1688)$ does decay into $K^+ + \Lambda$. Furthermore, there is also some indication that this isobar plays a dominant role in K^+ production in nucleon-nucleon collisions at 19 and 23 GeV/c.[19] So let us assume the following reaction:

$$p+p \rightarrow N^{*+}+p \qquad \searrow \; K^+ + \Lambda^0, \tag{3}$$

where N^* is the isobar of mass $M_0 = 1.688$ GeV/c^2 and width $\Gamma = 100$ MeV/c^2.

The total cross section for $N^{*+}(1688)$ production in p-p collisions is 1 mb at 3.17-GeV incident proton energy and 1.6 mb at 4.6 GeV.[17] The branching ratio for $N^{*+}(1688)$ decaying into $K^+ + \Lambda$ is $\sim 1\%$.[17,18] Therefore, at 3 GeV the total cross section for reaction (3) is expected to be 10 μb or less. Since our measured cross section at 3.03 GeV is 160 ± 29 μb (see Table II), we expect $\sim 10/160 \cong 6\%$ of the kaons to be produced through (3). If we try to fit our data to the momentum distribution which is expected when 6% of the events go through (3) and the rest through phase space, we obtain a very poor fit, irrespective of the angular distribution chosen for the N^* production. Even if we allow the contribution of (3) to be as high as 25%, the fit is still worse than the fits of Fig. 10. Consequently, this model does not seem to provide a likely explanation for the experimental observations.

E. One-Pion-Exchange Model

Our calculations for this well-known model (OPE) follow closely those of Ferrari and Selleri.[20]

We have considered only the two Feynman diagrams shown in Fig. 11 and have neglected interference terms.

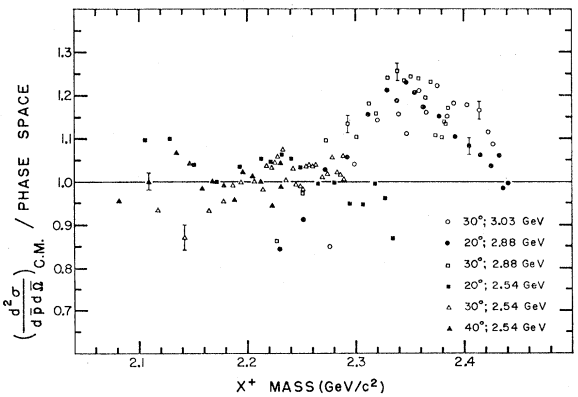

FIG. 9. Ratio of data to phase space as a function of the effective mass of $X^+(p+p \rightarrow K^+ + X^+)$. Only a few error bars are shown.

[14] S. J. Lindenbaum and R. M. Sternheimer, Phys. Rev. **105**, 1874 (1957); **106**, 1107 (1957); Phys. Rev. Letters **5**, 24 (1960); Phys. Rev. **109**, 1723 (1958); **123**, 333 (1961).

[15] J. Schwartz, D. H. Miller, G. R. Kalbfleisch, and G. A. Smith, Bull Am. Phys. Soc. **9**, 420 (1964).

[16] B. Musgrave, G. Petmezas, L. Riddiford, R. Böck, E. Fett, B. R. French, J. B. Kinson, Ch. Peyrou, M. Szeptycka, J. Badier, M. Bazin, L. Blaskovic, B. Equer, J. Huc, S. R. Borenstein, S. J. Goldsack, D. H. Miller, J. Meyer, D. Revel, B. Tallini, and S. Zylberajch, Nuovo Cimento **35**, 735 (1965).

[17] G. Alexander, O. Benary, G. Czapek, B. Haber, N. Kidron, B. Reuter, A. Shapira, E. Simopoulou, and G. Yekutieli, Phys. Rev. **154**, 1284 (1967).

[18] V. Alles-Borelli, B. French, Å. Frisk, and L. Michejda, Nuovo Cimento **47A**, 322 (1967).

[19] D. Dekkers, J. A. Geibel, R. Mermod, G. Weber, T. R. Willits, K. Winter, B. Jordan, M. Vivargent, N. M. King, and E. J. N. Wilson, Phys. Rev. **137**, B962 (1965).

[20] E. Ferrari and F. Selleri, Nuovo Cimento Suppl. **24**, 453 (1962).

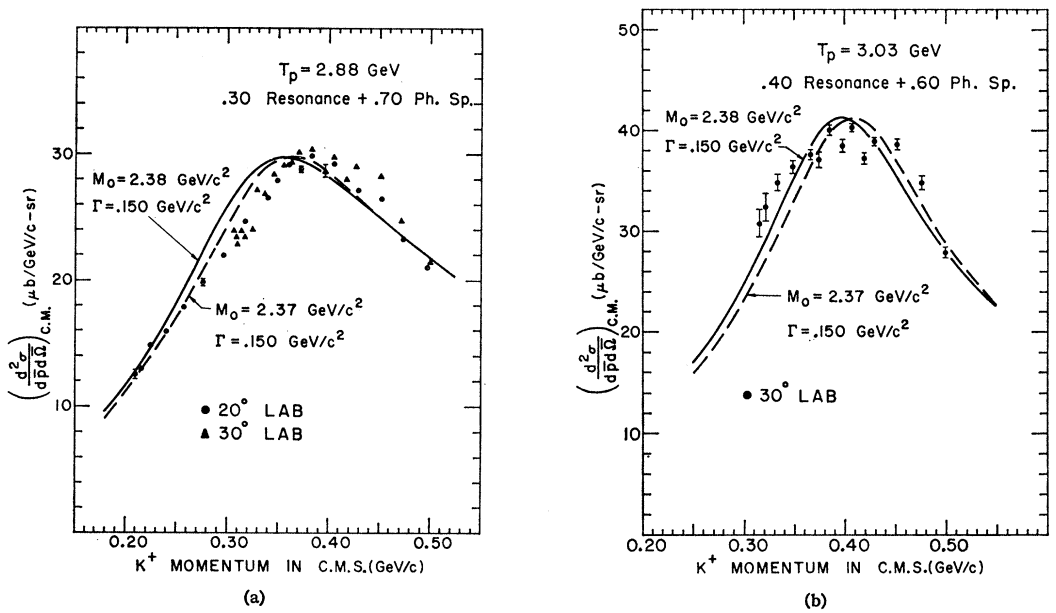

FIG. 10. Predictions of dibaryon model at 2.88 and 3.03 GeV. Curves are arbitrarily normalized to the area under the data.

For simplicity we have used the pole approximation which consists of setting the form factor of the three-pronged vertex equal to 1 and using the on-shell differential cross section for the four-pronged vertex. The implications of these approximations have been discussed by Ferrari and Selleri.[20,21] The differential cross section for the reaction $\pi^0+p\rightarrow\Lambda^0+K^+$ was assumed, on the basis of charge independence, to have the same dependence on energy and angle as the differential cross section for $\pi^-+p\rightarrow\Lambda^0+K^0$, namely $(d\sigma/d\Omega)_{\Lambda^0K^+}(\omega)=\frac{1}{2}(d\sigma/d\Omega)_{\Lambda^0K^0}(\omega)$. Much information is available on the latter reaction.[22,23]

In Fig. 12 we compare the OPE predictions with the data obtained at 2.54 GeV. For all three curves, only one arbitrary normalization factor has been used. It is clear that these fits are much worse than those predicted by phase space [Figs. 4(a)–4(c)].

Figure 13 shows the comparison between OPE and data at 2.88 and 3.03 GeV. Here again, only one arbitrary normalization factor has been used at each energy. As can be seen, the fits are not good either.

It should be mentioned that in the above calculations we have not considered the reaction $p+p\rightarrow K^+ +\Sigma+N$, because the reactions $\pi^0+p\rightarrow\Sigma^0+K^+$ and $\pi^-+p\rightarrow\Sigma^0+K^0$ cannot be directly related on the basis of charge independence (initial and final states contain a mixture of isotopic spin states). However, this omission should not be too significant since it is known[13] that the Λp and Σp effective-mass distributions have essentially the same shape.

In Table II we present, together with our data, the absolute total cross sections calculated by Ferrari[24] for both the OPE and OKE (one-kaon-exchange) models. The agreement is good for the OPE model, except at low energy, whereas the OKE predictions are too high by a factor of ~ 3.

V. SUMMARY AND CONCLUSIONS

In this paper we have presented the results of an experimental study of K^+-meson production in p-p colli-

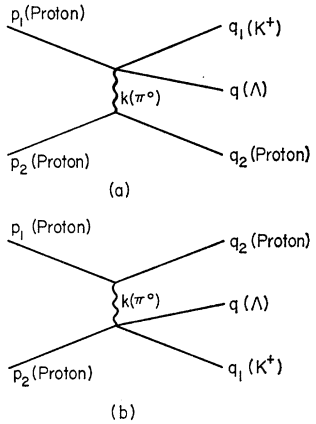

FIG. 11. Feynman diagrams for $p+p\rightarrow K^++\Lambda^0+p$ in the one-pion-exchange (OPE) model.

[21] E. Ferrari and F. Selleri, Phys. Rev. Letters **7**, 387 (1961); Nuovo Cimento **27**, 1450 (1963); **21**, 1028 (1961).

[22] J. A. Anderson, F. S. Crawford, B. B. Crawford, R. L. Golden, L. J. Lloyd, G. W. Meisner, and L. R. Price, in *Proceedings of the International Conference on High-Energy Physics, Geneva, 1962*, edited by J. Prentki (CERN Scientific Information Service, Geneva, 1962), p. 271.

[23] Joseph Keren, Phys. Rev. **133**, B458 (1964).

[24] E. Ferrari, Phys. Rev. **120**, 988 (1960); see also T. Yao, *ibid.* **125**, 1048 (1962).

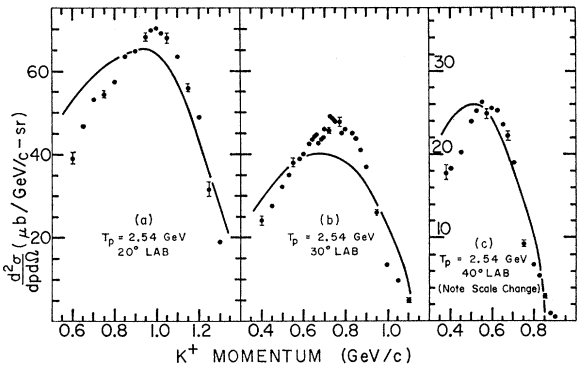

FIG. 12. OPE predictions at 2.54 GeV. Only one arbitrary normalization factor has been used for the three curves.

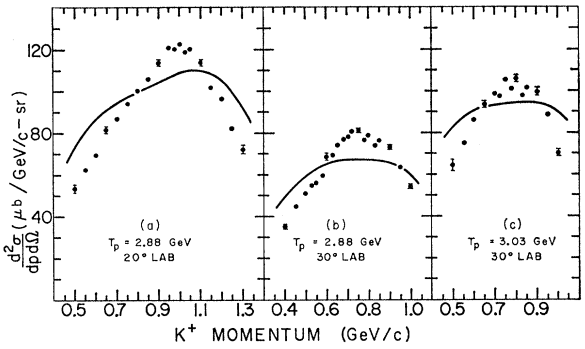

FIG. 13. OPE predictions at 2.88 and 3.03 GeV. Again only one arbitrary normalization factor has been used at each energy.

sions at 2.54, 2.88, and 3.03 GeV and at laboratory angles of 20°, 30°, and 40°.

The K^+ momentum spectra, transformed to the c.m. system, do not indicate any anisotropy over the angular range covered (60°–140°). Assuming that isotropy in the c.m. system holds for the entire sphere and at all three energies, we obtain the total cross sections for K^+ production presented in Table II. Our result at 2.88 GeV (123 ± 21 μb) is in good agreement with the cross section obtained by Louttit *et al.*[4] at 2.85 GeV (129 ± 20 μb), but does not agree as well with that reported by Melissinos *et al.*[5] at the same energy (181 ± 36 μb). Also, as explained in Sec. IV A, we find no evidence for any of the previously reported[5,11,12] *narrow* structures.

At 2.54 GeV, the experimental data are well described by phase space with 60% $K^+\Sigma N$ and 40% $K^+\Lambda p$ in the final state. At the two higher energies we confirm the earlier finding[2] that there is a definite disagreement with phase-space predictions.

In an attempt to interpret these results, we have compared our data with the predictions of three models: (1) a model based on the assumption that K's are produced in the reaction $p+p\rightarrow K^++X^+$, where X^+ is a $B=2$, $S=-1$ resonance which decays into a nucleon +hyperon; (2) the isobar model $[p+p\rightarrow N^{*+}(1688)+p$, followed by $N^{*+}(1688)\rightarrow K^++\Lambda^0]$; and (3) the one-pion-exchange model. We find the first model to be inconclusive because of too many free parameters. The isobar model is clearly inadequate. The one-pion-exchange model (as outlined in Sec. IV E) is moderately successful in predicting total cross sections (except at low energy); however, it does not give a good interpretation of the *detailed* experimental observations.

ACKNOWLEDGMENTS

We wish to thank the members of the staff of the Princeton-Pennsylvania accelerator for their constant support and cooperation throughout the experiment. We are grateful to Professor A. Lemonick and P. Kunz for the considerable help they provided at various stages of this project, and also to W. T. Ford for his assistance in the taking of the data. The credit for the excellent performance of the internal hydrogen target belongs to R. Jankowicz. Finally, we would like to acknowledge many valuable discussions with Professor S. Treiman.